Pola 1

The symmetry of a knot, which is our first aesthetic constraint, is determined by the number of moves to the right minus the number of moves to the left,

$$s = \sum_{i=1}^{h} x_i$$

where $x_i = 1$ if the ith step is $\hat{\mathrm{r}}$, -1 if the ith step is $\hat{\mathrm{l}}$ and 0 otherwise. Because asymmetric knots disrupt human bilateral symmetry, we consider the most symmetric knots from each class, that is, the ones that minimize s.

Whereas the centre number γ and the symmetry s specify the move composition of a knot, balance relates to the distribution of these moves; it corresponds to the extent to which the moves are mixed. A balanced knot is tightly bound and keeps its shape. We use this as our second aesthetic constraint. The balance b may be expressed as

$$b = (1/2)\sum_{i=2}^{h-1} |\omega_i - \omega_{i-1}|$$

and the winding direction $\omega_i(\sigma_i, \sigma_{i+1}) = 1$, where σ_i represents the ith step of the walk, if the transition from σ_i to σ_{i+1} is clockwise, say, and -1 otherwise. Of those knots that are optimally symmetric, we desire that knot which minimizes b.

The ten canonical knot classes $\{h, \gamma\}$ and the corresponding most aesthetic knots are listed in Table 1. The four named knots are the only ones, to our knowledge, to have received widespread attention, either published or through tradition. Here we introduce some unnamed knots.

The first four columns of Table 1 describe the knot class $\{h, \gamma\}$, whereas the remainder relate to the corresponding most aesthetic knot. The centre fraction γ/h provides a guide to the shape of a knot, with higher fractions corresponding to broader knots; along with the size h, it should be used in selecting a knot.

Some readers may notice the use of knots whose sequences are equivalent to those shown in Table 1 apart from transpositions of $\hat{\mathrm{r}}$, $\hat{\mathrm{l}}$ groups, such as the use of $L_{\otimes}\, R_{\odot}\, C_{\otimes}\, R_{\odot}\, L_{\otimes}\, C_{\odot}\, T$ in place of the half-Windsor (T. P. Harte and L. S. G. E. Howard, personal communication); some will argue that this *is* the half-Windsor. Such ambiguity follows from the variable width of conventional ties (the earliest ties were uniformly wide). This makes some transpositions arguably favourable, namely the last $\hat{\mathrm{r}}$, $\hat{\mathrm{l}}$ group in the knots {5, 2}, {6, 2}, {7, 2}, {8, 3} and {9, 3} in Table 1. We do not attempt to distinguish between these knots and their counterparts; this much we leave to the sartorial discretion of the reader.

Thomas M. Fink, Yong Mao
Cavendish Laboratory,
Cambridge CB3 0HE, UK
e-mail: tmf20@cus.cam.ac.uk

Pasture damage by an Amazonian earthworm

Almost all cultivated soils undergo some reduction in the porosity of the surface layers, and nowhere is this more evident than in tropical rainforests that have been converted to pastures. Following deforestation in an area of Costa Rica, soil bulk density has been shown to increase rapidly after conversion to pasture, leading to poor drainage and a reduced rate of gaseous diffusion[1]. These factors limit methane consumption and promote the anaerobic production of methane. A similar effect on methane flux has been found in upland soils in the Brazilian Amazonian basin after conversion from forest to pasture[2,3]. Increases in atmospheric methane are therefore not limited to emissions from flooded soils[4], as forest-to-pasture conversion promotes the anaerobic mineralization of organic matter by changing the physical properties of soil.

We now demonstrate the importance of this process in pasture degradation in central Amazonia, close to Manaus in northern Brazil (Fig. 1a). We show that, in addition to the substantial compacting effects of heavy machinery[5] and cattle trampling[6], another more insidious agent — the soil macrofauna — can have profound and lasting effects[7,8] on the porosity of pasture soils.

We wetted a natural forest soil (xanthic acrudox, USDA, 1996) to a water potential of -10 kPa and compressed it at a pressure of 10^3 kPa, measured using an oedometer. Macroporosity (in the range 0.1. to 100 μm) fell from 21.7 to 3 cm^3 per 100 g, indicating that forest surface soils (at a depth of 0–5 cm) are extremely sensitive to compaction (Fig. 1b). Passing the same soil through the gut of the earthworm *Pontoscolex corethrurus*, an aggressive exotic colonist that invades many tropical pastures, reduced macroporosity even more to 1.6 cm^3 per 100 g. We believe that this change is brought about by the intense mixing and near-complete dispersion of soil particles in the moist environment of the earthworm gut (water content: 0.85 g per g).

During conversion from forest to pasture, two separate mechanisms act to compact the soil. First, the effects of heavy machinery[5] and trampling by cattle[6] occur in specific locations and result from the techniques used for deforestation and pasture management. They lead to the mixing of plant debris and clay in the upper 5 cm and to severe compaction in the layer 5–10 cm deep (Fig. 1c). Second, the effects of reduced abundance and diversity of macrofaunal communities in the newly created pastures are linked to ecosystem dynamics

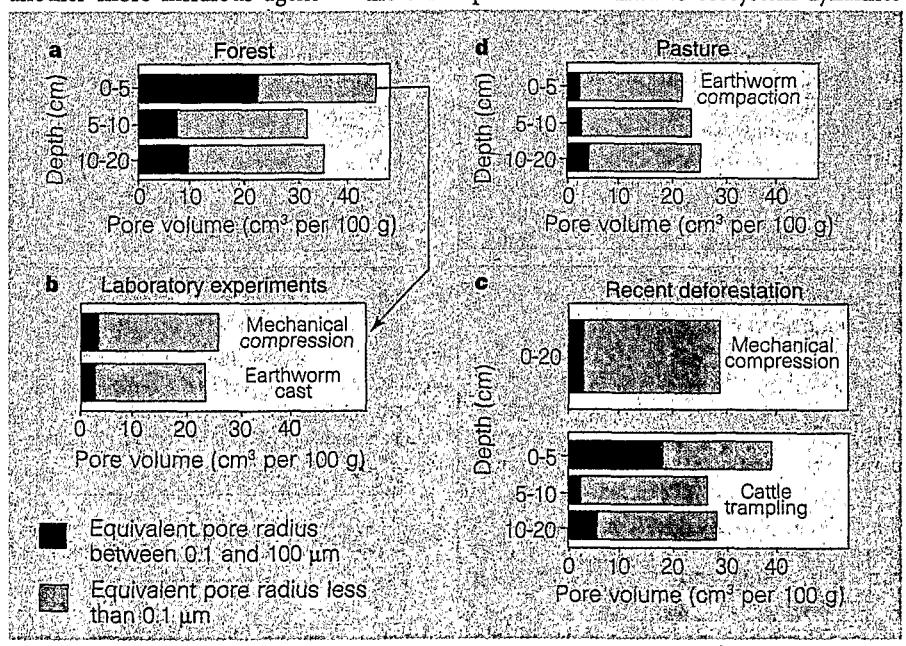

Figure 1 Effect of mechanical and biological action on soil pore distribution in central Amazonia. Data are deduced from mercury porosimetry analysis[10]. The pore size distribution shows a bimodal pattern, indicating that there are two types: the largest pores, which have an equivalent pore radius (EPR) between 0.1 and 100 μm, are biological in origin or are fine fissures, and are essential for gas exchange and the infiltration and retention of free water; the smaller pores, with an EPR of less than 0.1 μm, are found in compact clumps of kaolinite. **a,** In primary forest, biodiverse soil macrofauna and roots regulate soil pore volume. **b,** Laboratory experiments in which the forest surface horizon is compacted by mechanical compression (10^3 kPa) of soil with a water potential of -10 kPa, or by mechanical working and dispersion in the earthworm gut. **c,** Effects of recent deforestation due to heavy machinery and trampling by cattle (after manual clearance). **d,** Ungrazed, manually deforested pasture shows accumulation of compact surface casts in the layer 0–5 cm deep.

Fonds Documentaire ORSTOM
Cote : B*17164 Ex : 1 n°6722
Fonds Documentaire ORSTOM

and so are widespread and long-lasting. While the forest remains undisturbed, a highly diverse soil macrofauna maintains an adequate soil pore volume by balancing the effects of compacting and decompacting agents[7] (Fig. 1a). However, deforestation and the establishment of exotic grasses lead to a dramatic fall in biodiversity: 68% of the soil macrofaunal taxa of the original forest disappear and are replaced by large populations of the earthworm *P. corethrurus* (to a maximum of 400 per m^2).

These earthworm populations can make up nearly 90% of soil invertebrate biomass, and produce more than 100 tonnes per hectare per year of casts, dramatically decreasing macroporosity to 2.7 cm^3 per 100 g, a level as low as that found after the compaction of moist soils by heavy machinery. During the rainy season (November to June), intense casting by *P. corethrurus* at the surface of the saturated soil leads to the formation of a large continuous grey mass of casts 5 cm thick with a water content as high as 0.65 g per g. While the soil remains moist, this muddy layer has a continuous water phase that impedes gas exchange between the soil and the atmosphere. The resulting anaerobic soil conditions lead to the increased production of methane and limit its consumption. At the end of the rainy season, desiccation cracks form in the drying soil and the planted pastures wilt.

The best way to restore soils with this type of degraded structure is to maintain or establish enough woody plants in the landscape[9] to support an adequately diverse macro-invertebrate fauna.

Armand Chauvel*, Michel Grimaldi†, Eleusa Barros‡, Eric Blanchart§, Thierry Desjardins*, Max Sarrazin‡, Patrick Lavelle*

**Laboratoire d'Ecologie des Sols Tropicaux, ORSTOM, 32 avenue Henri Varagnat, 93143 Bondy Cedex, France*
e-mail: chauvel@bondy.orstom.fr
†ORSTOM/INRA, Science du Sol, 65 rue de St Brieuc, 35000 Rennes, France
‡INPA/ORSTOM–Ecologia, CP 478, 69011-970, Manaus AM, Brazil
§ORSTOM Martinique, BP 8002, 97259 Fort de France, France

1. Keller, M., Veldkamp, E., Weltz, A. M. & Reiners W. A. *Nature* 365, 244–246 (1993).
2. Steudler, P. A. *et al. J. Geophys. Res.* 101, 18547–18554 (1996).
3. Luizao, F., Matson, P., Luizao, R. & Vitousek, P. *Global Biogeochem. Cycles* 3, 281–285 (1989).
4. Seiler, W. & Conrad, R. in *The Geophysiology of Amazonia. Vegetation and Climate Interactions* (ed. Dickinson, R. E.) 133–162 (Wiley, New York, 1987).
5. Chauvel, A., Grimaldi, M. & Tessier, D. *Forest Ecol. Mgmt* 38, 259–274 (1991).
6. Grimaldi, M. *et al. Cahiers Agric.* 2, 36–47 (1993).
7. Blanchart, E., Lavelle, P., Braudeau, E., Le Bissonais, Y. & Valentin, C. *Soil Biol. Biochem.* 29, 431–439 (1997).
8. Alegre, J. C., Pashanasi, B. & Lavelle, P. *Soil Sci. Soc. Am. J.* 60, 1522–1529 (1996).
9. Ramachandran Nair, P. K. in *An Introduction to Agroforestry* 261–343 (Kluwer, 1993).
10. Lawrence, G. P. *J. Soil Sci.* 28, 527–540 (1977).

Using hair to screen for breast cancer

We have studied hair using fibre X-ray diffraction studies with synchrotron radiation and find that hair from breast-cancer patients has a different intermolecular structure to hair from healthy subjects. These changes are seen in all samples of scalp and pubic hair taken from women diagnosed with breast cancer. All the hair samples from women who tested positive for a mutation of the *BRCA1* gene, which is associated with a higher risk of breast cancer[1], also show these changes. Because our results are so consistent, we propose that such hair analyses may be used as a simple, non-invasive screening method for breast cancer.

We previously examined the intermolecular structure of normal human hair by using synchrotron X-ray scattering on multiple fibres[2,3]. The change in the hair from breast-cancer patients can be seen in the X-ray diffraction pattern as one or more rings of intensity that superimpose on the pattern for normal hair (Fig. 1). We believe that this pattern arises from a variation in the structure of the cell membrane as the hair is formed in the follicle.

We performed four studies on hair from controls and from patients with breast carcinoma. The first double-blind study (samples provided by A. Howell, Christie CRC Research Centre, Manchester) was carried out on beamline 15A at the Photon Factory (Japan). After correlating the diffraction patterns with patient data, we considered that the changes might indicate a propensity to malignancy and be related to breast cancer *per se*. To test this idea, we did another double-blind study on a larger sample of hair from the same source. This time, the X-ray measurements were made on the Australian National Beamline Facility and later confirmed on the BioCAT beamline at the Advanced Photon Source (Chicago).

The initial results showed some inconsistencies, which were eliminated when we excluded hair samples that had been 'permed' less than three months before collection. To avoid problems caused by hair treatment, we used samples of pubic hair collected at the Oncology Unit, St George Hospital (Sydney, Australia).

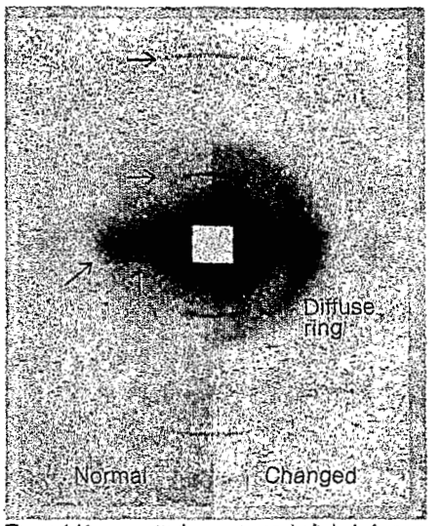

Figure 1 X-ray scattering patterns. Left, hair from a healthy 21-year-old female; right, hair from a 48-year-old breast-cancer patient. Horizontal and vertical arrows, parts of the pattern that are unchanged and arise from ordering and packing in the hair fibril. Diagonal arrow, a region of intensity arising from the membrane bonding the fibrils together. In the changed pattern, a diffuse ring resulting from random orientation superimposes on this region.

All hair samples (23 out of 23) taken from breast-cancer patients exhibited the characteristic change in their X-ray scattering patterns (Table 1). Of the samples taken from patients not suspected of having breast cancer, the scattering patterns of 86% (24 out of 28) were normal. In addition, of those not yet diagnosed with breast cancer but suspected of being at risk (because of familial history and the presence of a pathological mutation of *BRCA1*), 60% (3 out of 5) showed the full change associated with breast carcinoma; the remainder showed a partial change.

The ring that characterizes the hair from breast-cancer patients corresponds to a molecular spacing of 4.44 ± 0.06 nm, which places it directly in the position of the equatorial arc representing the plasma membrane in the normal hair pattern. The ring probably arises from randomly orientated lipid bilayers, either in the plasma membrane or in membranous inclusions in the hair cells, but this needs further study.

We correctly identified all the samples from women with breast cancer, but further

Table 1 **Correlation of breast cancer with hair structure**

Breast cancer diagnosed?	Samples	Samples with changed structure	Familial history of cancer (pathologic *BRCA1* mutation)	Hair origin
Yes	15	15	Yes (positive)	Scalp
Yes	8	8	None	Pubic
No	3	3	Yes (positive)	Scalp
No	2	Partial 2	Yes (positive)	Scalp
No	8	1	Yes (negative)	Scalp
No	16	3	None	Scalp
No	4	0	None	Pubic